Optimization-based Controller Design for Rotorcraft

N.-K. Tsing[1], M.K.H. Fan[2], J. Barlow[3], A.L. Tits[1], M.B. Tischler[4]

Abstract

An optimization-based methodology for linear control system design is outlined by considering the design of a controller for a UH-60 rotorcraft in hover. A wide range of design specifications is accounted for: internal stability, decoupling between longitudinal and lateral motions, handling qualities and rejection of wind gusts, while taking into account physical limitations in the swashplate displacements and rates of displacement. The methodology crucially relies on user-machine interaction for tradeoff exploration.

1. Introduction

Airframe concepts for future rotorcraft such as the light attack helicopter (LHX) include high effective hinge offset rotors and multiple control effectors to maximize maneuverability. This and other possible features lead to a high level of bare airframe instability, control cross coupling, and control redundancy. At the same time there is a need to include explicitly in a design methodology numerous specifications on control limits, actuator capabilities, cross coupling limits, and handling qualities. The classical control techniques which have been the primary tools of the industry are not well suited for such complex combinations. There is a great need for improved techniques. Numerous modern control methodologies have recently been proposed for application to these types of problems(e.g., [1-3]). However these studies have not adequately accounted for the many practical implementation problems of rotorcraft [4]. Key concerns in evaluating prospective modern control designs are the interaction of the rotor system dynamics [5] and the explicit inclusion of the complex design specifications(Mil-Specs [6]) in the design process.

A methodology is proposed that can account for various types of concurrent specifications: stability, decoupling between longitudinal and lateral motions, handling qualities, and physical limitations of the swashplate motions. This is achieved by synergistic use of analytical techniques (Q-parametrization of all stabilizing controllers, transfer function interpolation) and advanced numerical optimization techniques. The proposed methodology includes a two-parameter controller with separate consideration of the feedforward and the feedback portions. Preliminary results on the input/output part of the design were reported in [7], where a 21-state model was used for the aircraft. Here overall results are reported on

[1]Department of Electrical Engineering and Systems Research Center, University of Maryland, College Park, MD 20742.

[2]School of Electrical Engineering, Georgia Institute of Technology, Altanta, GA 30332

[3] Department of Aerospace Engineering, University of Maryland, College Park, MD 20742

[4]Ames Research Center, Moffett Field, CA 94035

a 37-state model generated by the UM-GenHel [8] nonlinear simulator. Nonlinear validation is also presented.

A central tool in this study was the interactive optimization-based package CONSOLE [9,10]. CONSOLE handles multiple (competing) objective functions, and constraints can be "soft" (moderate violations are allowed) or "hard". Specifications can be "functional", i.e., involve an entire time- or frequency-response rather than a single time or frequency point. For each specification, the designer provides a "good value" and a "bad value" (a "good curve" and a "bad curve" in case of a functional specification) and these can be interactively adjusted as tradeoffs are identified.

In Section 2 below, we briefly describe a simplified model of a rotorcraft in hover (based on the UH-60). In Section 3, a set of design specifications is proposed. In Section 4, the design methodology is outlined. In Section 5, some results are presented, including validation on the nonlinear model. Section 6 is devoted to some final remarks.

2. A Linearized Model for an UH-60 in Hover

The model we used for controller design, denoted by $P_0(s)$, is a 39-state linear model generated from UM-GenHel. UM-GenHel, developed at the Aerospace Engineering Department of the University of Maryland, is a nonlinear flight simulation program for helicopters [8]. It models the high order dynamics (such as main rotor blade motions and main rotor inflow) of the helicopter, and can generate linearized models of the helicopter at various flight conditions. The last six states of this linearized model correspond to hidden modes associated with the engine dynamics. These six states were removed from the model, leaving a 33-state minimal realization of $P_0(s)$. This realization has one pole at zero and a pair of real poles in the open right-half plane. It is non-minimum phase and strictly proper. In each of the four channels, the control system actuator is modeled by a first order Padé approximation corresponding to a 0.050 second delay. This yields a final count of 37 states.

An overall block diagram of the closed-loop system is represented in Figure 1. The four variables of the input $\delta_s = (\delta_{s\phi}, \delta_{s\theta}, \delta_{sc}, \delta_{s\psi})$ of $P_0(s)$ represent respectively the lateral, longitudinal, and collective displacements of the swashplate, and the position of the tail rotor actuator. The output is $y = (u, v, w, p, q, r, \phi, \theta, \psi)$, the variables of which stand for longitudinal velocity (u), lateral velocity (v), vertical velocity (w), roll rate (p), pitch rate (q), yaw rate (r), roll angle (ϕ), pitch angle (θ), and yaw angle (ψ). The delay block $D_e(s)$ has 4 states, 4 inputs, and 4 outputs. The command input $\delta = (\delta_\phi, \delta_\theta, \delta_c, \delta_\psi)$ consists of

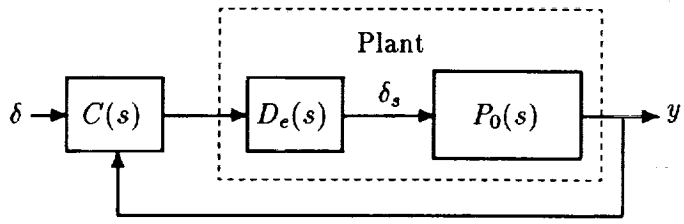

Figure 1: Control system configuration

roll command (δ_ϕ), pitch command (δ_θ), collective command (δ_c), and yaw command (δ_ψ). The rotorcraft is to be controlled by a two-parameter controller $C(s)$.

3. Design Specifications

A wide range of specifications, in both the time- and frequency domains, are to be satisfied. First, the closed-loop system must be internally stable. Second, to the extent possible, it is desired that the various longitudinal and lateral modes be decoupled and approximate specified step responses (handling quality specifications). Specifically, the pitch command should mostly affect the pitch angle (and pitch rate) and the longitudinal velocity; the collective command should mostly affect vertical velocity; the roll command should mostly affect the roll angle (and roll rate) and the lateral velocity; and the yaw command should affect mostly the yaw angle (and yaw rate). The "diagonal" responses should exhibit desirable characteristics as given in [6]. Third, the displacement and rate of displacement of the swashplate may not violate some physical limitations. Lastly, the closed-loop system should exhibit good performance in gust rejection. The mathematical formulation of these specifications is described below. (Note: all inputs are expressed in inches of stick.)

Spec 1 The closed-loop system is internally stable.

Spec 2 When the input $\delta = [0 \;\; 5 \;\; 0 \;\; 0]^T$:

Spec 2.1 Pitch response $\theta(t)$ should lie between the two curves $C_1(t)$ and $C_2(t)$ of Figure 2.

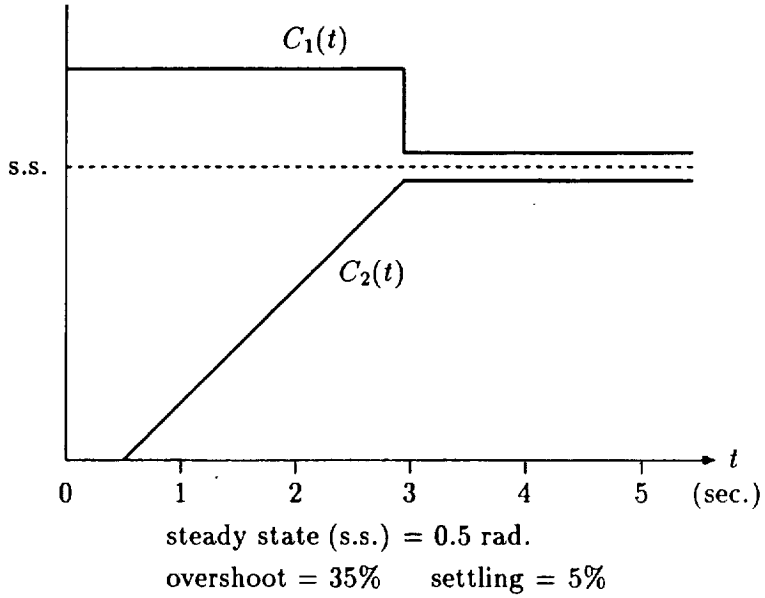

Figure 2: Boundaries for pitch response

Spec 2.2 Decoupling: (i) $\phi(t)$, $\psi(t)$ should have the absolute values less than 5% of $\theta(5)$ for $t \in [0, 5]$; (ii) $v(t)$, $w(t)$ should have the absolute values less than 5% of $u(5)$ for $t \in [0, 5]$.

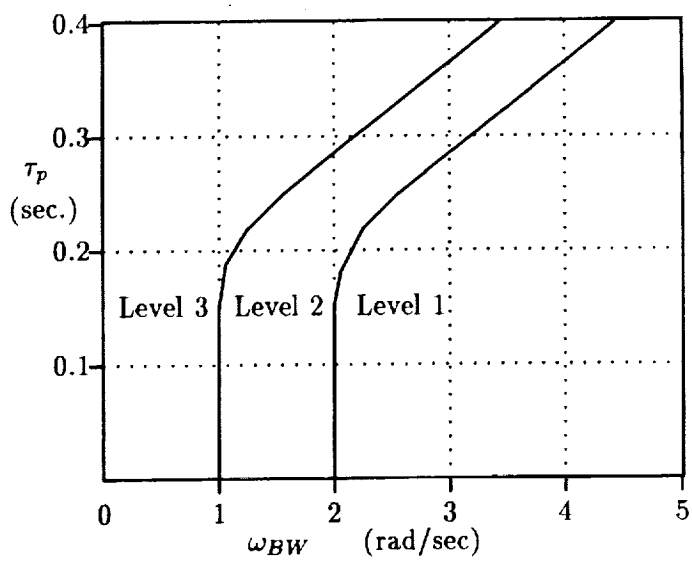

Figure 3: Handling quality specification

Spec 2.3 Physical limitations on swashplate displacements: the absolute values of $\delta_{s\theta}(t) + \delta_{sc}(t), \delta_{s\theta}(t) + \delta_{s\phi}(t), \delta_{s\phi}(t) + \delta_{sc}(t), \delta_{s\phi}(t), \delta_{s\theta}(t), \delta_{sc}(t)$, and $\delta_{s\psi}(t)$ should all be less than 10 inches for $t \in [0, 5]$.

Spec 2.4 Limitations on the velocities of the swashplate motion: the absolute values of $\dot{\delta}_{s\theta}(t) + \dot{\delta}_{sc}(t), \dot{\delta}_{s\theta}(t) + \dot{\delta}_{s\phi}(t), \dot{\delta}_{s\phi}(t) + \dot{\delta}_{sc}(t), \dot{\delta}_{s\phi}(t), \dot{\delta}_{s\theta}(t), \dot{\delta}_{sc}(t)$, and $\dot{\delta}_{s\theta}(t)$ should all be less than 10 inches per second for $t \in [0, 5]$.

Spec 3 Let H_θ be the transfer function from δ_θ to θ. Suppose ω_{BW} (bandwidth) and τ_p (phase delay) are defined based on the Bode plot (phase part) of H_θ, such that ω_{BW} is the frequency corresponding to 45 degree phase margin, and phase delay τ_p is defined as

$$\tau_p = -\frac{\Phi_{2\omega_{180}} + 180}{\frac{360}{2\pi} \times 2\omega_{180}}$$

where ω_{180} is the frequency at which the phase angle attains -180 degree, and $\Phi_{2\omega_{180}}$ is the phase angle at frequency $2\omega_{180}$ (see [4]). Then the graph of (ω_{BW}, τ_p) should lie within region Level 1 in Figure 3.

Spec 4 When the input $\delta = [5 \ 0 \ 0 \ 0]^T$:

Spec 4.1 Roll response $\phi(t)$ should lie between the two curves $C_1(t)$ and $C_2(t)$ of Figure 2, with s.s.= 1 rad.

Spec 4.2 Decoupling: (i) $\theta(t)$, $\psi(t)$ should have the absolute values less than 5% of $\phi(5)$ for $t \in [0, 5]$; (ii) $u(t)$, $w(t)$ should have the absolute values less than 5% of $v(5)$ for $t \in [0, 5]$.

Spec 4.3 Physical limitations on swashplate displacements: same as spec 2.3.

Spec 4.4 Limitations on the speed of swashplate motion: same as spec 2.4.

Spec 5 Same as Spec 3 with H_θ replaced by H_ϕ, the transfer function from δ_ϕ to ϕ.

Spec 6 When input = [0 0 0 2.5] :
Spec 6.1 Yaw rate $r(t)$ should lie between the two curves $C_1(t)$ and $C_2(t)$ of Figure 2, with s.s.= 0.4 rad/sec.
Spec 6.2 Decoupling: $p(t)$, $q(t)$ should have the absolute values less than 5% of $r(5)$ for $t \in [0,5]$.
Spec 6.3 Physical limitations on swashplate displacements: same as spec 2.3.
Spec 6.4 Limitations on the speed of swashplate motion: same as spec 2.4.

Spec 7 Same as Spec 3 with H_θ replaced by H_ψ, the transfer function from δ_ψ to ψ.

Spec 8 When input = [0 0 5 0] :
Spec 8.1 Vertical velocity $w(t)$ should satisfy

$$\mathcal{L}^{-1}\left[\frac{5Ke^{-\tau s}}{s(Ts+1)}\right](t) \le w(t) \le 1.1\,\mathcal{L}^{-1}\left[\frac{5Ke^{-\tau s}}{s(Ts+1)}\right](t) + 2$$

for all $t \in [0,5]$, where $K = 10$, $\tau = 0.2$, $T = 5$, and $\mathcal{L}^{-1}$ denotes the inverse Laplace transform.
Spec 8.2 Decoupling: $u(t)$, $v(t)$ should have the absolute values less than 5% of $w(5)$ for $t \in [0,5]$.
Spec 8.3 Physical limitations on swashplate displacements: same as spec 2.3.
Spec 8.4 Limitations on the speed of swashplate motion: same as spec 2.4.

Spec 9 A wind gust, which is modeled by the step response of

$$g(s) = \frac{0.44s}{(s+1)^2}, \qquad \text{(gust model)} \tag{1}$$

is to be injected at the output nodes ϕ, θ, and ψ in turn.
Spec 9.1 The closed-loop transient response at the corresponding node, when the wind gust is injected, should be kept within the envelope of the step response of

$$h_{\text{allow}}(s) = \frac{0.155s}{s^2 + 1.77s + 0.462}. \tag{2}$$

Step responses of $g(s)$ and $h_{\text{allow}}(s)$ are shown in Figure 4.
Spec 9.2 Physical limitations on swashplate displacements, same as spec 2.3, but time interval is changed to $[0,\infty)$.
Spec 9.3 Limitations on the speed of swashplate motion, same as spec 2.4, but time interval is changed to $[0,\infty)$.

We remark that, given the highly coupled dynamics of the plant ($P_0(s)$), these specifications are very stringent, and to our knowledge no controller has been built so far that satisfies all these specifications.

The asymmetry of the rotorcraft places fundamental limitations on the amount of decoupling that can be achieved between the various channels. The most striking instance is the impossibility of maintaining a constant nonzero pitch angle without steady state banking. For the linear model used in this study, it can be verified (see [11,12] for details) that the minimum achievable ratio between steady state roll and pitch angles is slightly over

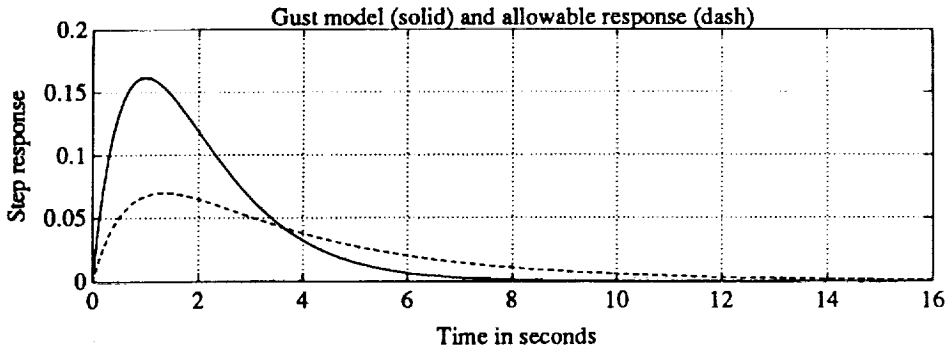

Figure 4: Gust model and allowable closed-loop response

20%. Note however that this does not preclude the possibility of meeting specification 2.2 as it requires significant decoupling over the first 5 seconds only. Yet, this limitation ought to be kept in mind when interactively exploring possible tradeoff designs.

4. Methodology

Design of a two-parameter controller proceeds as follows [13]. First the overall aircraft transfer matrix (rotor + airframe dynamics + delay) $P(s) = P_0(s)D_e(s)$ is factorized over the ring of stable transfer functions, i.e.,

$$P(s) = N(s)D^{-1}(s) = \tilde{D}^{-1}(s)\tilde{N}(s)$$

where $N(s)$, $D(s)$, $\tilde{N}(s)$ and $\tilde{D}(s)$ are stable transfer matrices, $(N(s), D(s))$ are right coprime and $(\tilde{N}(s), \tilde{D}(s))$ are left coprime. Next let $X(s)$ and $Y(s)$ be stable transfer matrices satisfying the Bezout identity

$$X(s)N(s) + Y(s)D(s) = I$$

Then all stabilizing controllers can be obtained according to the block diagram of Figure 5 where both $Q(s)$ and $R(s)$ range over the class of all stable transfer matrices of appropriate dimension (with the condition that $\det(Y(s) - R(s)\tilde{N}(s))$ does not vanish identically).

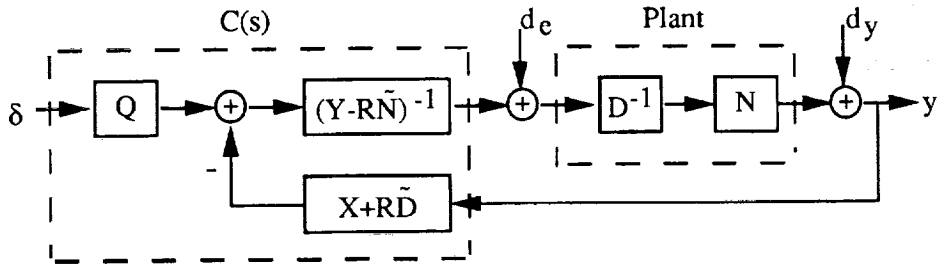

Figure 5: Two-parameter controller

It is easily verified that the overall transfer function $T(s)$ from δ to y is given by

$$T(s) = N(s)Q(s) \tag{4.1}$$

while the transfer function from δ to the swashplate displacements δ_s by

$$S(s) = D_e(s)D(s)Q(s) \tag{4.2}$$

Thus both are independent of the R parameter. On the other hand the transfer function from disturbance inputs d_e and d_y to those same outputs y and δ_s is given by

$$\begin{bmatrix} D(s)(Y(s) - R(s)\tilde{N}(s)) & -D(s)(X(s) + R(s)\tilde{D}(s)) \\ N(s)(Y(s) - R(s)\tilde{N}(s)) & -N(s)(X(s) + R(s)\tilde{D}(s)) + I \end{bmatrix}$$

which is independent of the Q parameter. By adopting the two-parameter controller structure, the control designer can then separate the design problem into two independent subproblems of input/output performance (to be solved by choosing a "good" Q: Q-design) and of disturbance rejection (to be solved by choosing a "good" R: R-design), respectively. At the same time, internal stability will be automatically guaranteed if the chosen $Q(s)$ and $R(s)$ are stable.

Q-design

We just saw that any stable $Q(s)$ yields a stable $T(s)$ and any stable $T(s)$ corresponds to a stable $Q(s)$, so that this "Q-parameterization" automatically takes care of specification 1. Concerning the other input/output specifications, the structure of the problem allows another major simplification. Note that each one of the specifications 2-8 involved only one of the four input channels and (see (4.1-2)) each column of $Q(s)$ affects the I/O transfer function corresponding to exactly one input channel (i.e., exactly one column of $Q(s)$). As a result the problem can be decomposed into four optimization problems, each one involving a single column of $Q(s)$ and the specifications involving inputs corresponding to that column. Thus, interactive optimization will be used, for each input channel, to try to satisfy the corresponding input/output specifications; this will involve a single column of $Q(s)$, which we will denote by $q(s)$.

A possible parametrization for $q(s)$, once its McMillan degree n has been chosen, is by writing

$$q(s) = C(sI - A)^{-1}B + D \tag{4.3}$$

with

$$A = \begin{bmatrix} 0 & 1 & & & & & \\ p_1 & p_2 & & & & & \\ & & 0 & 1 & & & \\ & & p_3 & p_4 & & & \\ & & & & \ddots & & \\ & & & & & 0 & 1 \\ & & & & & p_{2j-1} & p_{2j} \end{bmatrix}, \quad B = \begin{bmatrix} 1 \\ 0 \\ 1 \\ 0 \\ \vdots \\ 1 \\ 0 \end{bmatrix} \tag{4.4a}$$

if $n = 2j$ is even, and

$$A = \begin{bmatrix} 0 & 1 & & & & \\ p_1 & p_2 & & & & \\ & & \ddots & & & \\ & & & 0 & 1 & \\ & & & p_{2j-1} & p_{2j} & \\ & & & & & p_{2j+1} \end{bmatrix}, \quad B = \begin{bmatrix} 1 \\ 0 \\ 1 \\ 0 \\ \vdots \\ 1 \end{bmatrix} \tag{4.4b}$$

if $n = 2j + 1$ is odd, and using the p_i's as well as all entries of C and D as free parameters. Indeed, it is clear that by constraining the p_i's to be negative, only stable $Q(s)$ will be generated; it is also easy to show that the family of matrices $Q(s)$ thus generated is open and dense in the set of stable matrices of McMillan degree n.

One difficulty with the parametrization just proposed is the ensuing large number of design parameters, resulting in (i) large computation times and (ii) likeliness that a local rather than global optimum be reached. The following heuristics drastically reduces the number of design parameters by eliminating a large portion of "clearly nonoptimal" $q(s)$ and likely retaining enough of the "good" ones to allow a "close to optimal" $q(s)$ to be identified. For given A and B (i.e., given p_i's) and given "sampling frequencies" $\omega_1, \ldots, \omega_\ell$ (the p_i's and the ω_i's will be the design parameters) corresponding C and D are selected by solving, in a least square sense,

$$N(j\omega_i)(C(j\omega_i I - A)^{-1}B + D) = T(j\omega_i), i = 1, \ldots, \ell \tag{4.5}$$

where $T(s)$ is an approximate "desired" transfer function constructed from the specifications: good "diagonal" responses and "off diagonal" responses set to zero. (The method that was actually used is somewhat more sophisticated in that it involves solving two successive linear least squares problems: see [11,12].)

To summarize, the numerical optimization process will proceed as follows. Given values of the p_i's and ω_i's (design parameters), $q(s)$ will be obtained by solving for C and D the linear least square problem; time and frequency responses of the closed-loop system will be computed (by invoking MATLAB); the values of the specifications and their gradients (with respect to the design parameters) will be determined; the optimization algorithm (the heart of CONSOLE) will use this information to select new values of the design parameters; and the cycle will start again until the designer decides to interrupt it. The designer can then relax or tighten selected specifications in order to explore various tradeoffs.

In addition to the specifications outlined in Section 3, it may be desired to achieve or approach certain steady state values when unit steps are fed into individual channels. In view of the Final Value theorem, these values are determined by $Q(0)$. The best value Q_* for $Q(0)$ can be determined, again, by solving a linear least squares problem. Let q_* be a column of Q_*. Then, in view of (4.3), we may require that

$$C(-A)^{-1}B + D = q_*,$$

i.e.,

$$D = q_* + CA^{-1}B.$$

Substituting this expression for D in (4.5) we obtain a linear least squares problem in C only. Note that, in the design results reported below, there was no such steady state requirement.

R-design

A major difference with the Q-design is that the columns of $R(s)$ cannot be designed independently, as each of these columns may affect all disturbance rejection specifications. Thus a parametrization of the form (4.3-4), where C and D are obtained by solving a linear system of the form (4.6) in the least squares sense, is used for the entire matrix $R(s)$.

5. Results and Validation

Based on our Q-design results, it is found that in the lateral, longitudinal, and tail collective channels, the swashplate rate specifications (Specs 2.4, 4.4, 6.4) are competing with the handling quality (based on frequency response) specifications (Specs 3, 5, 7). Specifically, for the handling quality indicator (ω_{BW}, τ_p) to lie within region Level 1 in Figure 3, the swashplate rates will attain magnitude above 10 inch/sec within the first 0.1 second. For example, Figure 6 and Figure 7 show the results of a design of the second column of Q (the longitudinal channel) on Specs 2.4 and 3. For this design, Spec 2.4 is satisfied but Spec 3 is not. Figure 8 and Figure 9 show the results of another design of the same column of Q on Specs 2.4 and 3. For this design, Spec 3 is satisfied but Spec 2.4 is not.

Our R-design results are that Specs 9.2 and 9.3 are satisfied, but Spec 9.1 is not. Figure 10 shows the response of the roll angle $\phi(t)$ (or, respectively, the pitch angle $\theta(t)$, or the yaw angle $\psi(t)$) when a wind-gust, modeled by the step response of $0.44s/(s+1)^2$, is injected at the roll angle node (or, respectively, the pitch angle node or the yaw angle node). From the figure, one sees that the graphs of the response do not lie within the allowable envelope given in Spec 9.1. Hence Spec 9.1 is not satisfied. The figure also suggests that the helicopter cannot act fast enough to respond to the gust, and can counteract the gust only after 0.3 second.

We finally choose a design of the controller for which the specifications on swashplate rates (Specs 2.4, 4.4, and 6.4) are satisfied but the handling quality specifications (Specs 3, 5, and 7) are not. This controller has 152 states. It is then reduced to 82 states via the balanced realization method. It has been examined, by checking against the specifications, that the performance of the order-reduced controller on the linearized model is as good as the unreduced, 152-state controller. This order-reduced controller is tested on both the UM-GENHEL linear and nonlinear simulation program. Based on the comparison between the open-loop time responses (to a step input) of the nonlinear and the linearized model, it is found that the nonlinearity of the helicopter model is very high.

Figure 11 shows some of the relevant time responses of the closed-loop (linear and nonlinear) systems, when a 5 unit (in terms of inches of stick command) step command input is put on the lateral channel (δ_ϕ) of the controller. One notices from this figure that, after 2.5 seconds, the closed-loop responses of the nonlinear model do not match those of the linear model very well. However, given the high nonlinearity of the dynamics of the nonlinear model, this phenomenon should be expected. For example, Figure 11 shows that at 2.5 seconds after the control command has been issued, the roll angle of the nonlinear model is about 1 radian. This flight condition is very different from hover, and hence the dynamics of the nonlinear model at this point may be very different from that of the

linearized model for hover.

One would expect the discrepancies between the response of the closed-loop nonlinear system and that of the linear system should be less, if the magnitude of the control input is lowered. Figure 12 gives the comparison between the relevant responses of the nonlinear and linearized model, when the magnitude of the command input is lowered to 1. This clearly confirms that the response of the nonlinear model matches better with that of the linear model than before.

Finally, closed-loop responses of both the nonlinear and linear model, due to gust disturbance, are examined. For example, Figure 13 shows the roll angle response when gust is injected at the roll angle node. Notice that there are some discrepacies between the roll angle responses of the linear and the nonlinear model.

6. Discussion

The controller discussed in Section 5 is but one of the many sub-optimal controllers obtained when running CONSOLE. Indeed, a key advantage of an interactive package such as CONSOLE is that it allows the designer to explore alternative solutions by fine tuning the various target responses (this is especially so with CONSOLE's not yet released graphical interface).

It turns out that even the stability specification is amenable to tuning. Indeed, as discussed in [13], the Q-parametrization approach can be extended to generalized stability, i.e., confinement of closed loop poles in a more general region Π of the complex plane. This can be achieved by (i) factoring $P(s)$ in the ring of Π-stable (rather than Hurwitz stable) transfer functions and (ii) take for $Q(s)$ and $R(s)$ any matrices with all their poles in Π. The latter can be accomplished by suitably modifying parameterization (4.4). E.g., if Π is as in Figure 14, it suffices to replace in (4.4) 2×2 blocks of the form

$$\begin{bmatrix} 0 & 1 \\ p_1 & p_2 \end{bmatrix}$$

by

$$\begin{bmatrix} 0 & 1 \\ (1-y)(b-x)^2 - x^2(yk^2+1) & 2x \end{bmatrix}$$

and let x and y vary over $[(a+b)/2, b]$ and $[0,1]$, respectively (see [11,12] for details).

Finally, the merits of the approach discussed in this paper should be compared to those of the convex optimization approach proposed by S.P. Boyd and C.H. Barratt [14]. The main advantage of the latter is that it always yields the globally optimal design for the given specifications (for $Q(s)$ and $R(s)$ ranging over a finite dimensional subspace of the space of stable transfer matrices). A crucial requirement, however, is that all specifications be convex (as functions of the closed loop transfer matrix). It turns out that some of the specifications considered in the present study (in particular handling quality specifications such as Spec 3) do not satisfy this requirement (see [11,12] for details). Compared to the Ritz parameterization used in [14], while parameterization (4.3-4) would destroy any existing convexity, it has the advantage to cover all (in fact, "almost all") stabilizing controllers of a given degree.

Acknowledgement

This work was supported in part by NASA-Ames University Consortium Interchange No. NCA2-309, NSF Engineering Research Center Program No. NSFD-CDR-88-03012, and by NSF Grant No. DMC-84-51515.

References

[1] R.D. Holdridge, W.S. Hindson & A.E. Bryson, "LQG-Design and Flight Test of a Velocity-Command System for a Helicopter," *AIAA Guidance and Control Conference* (1985).

[2] W.L. Garrard & B.S. Liebst, "Design of a Multivariable Helicopter Flight Control System for Handling Qualities Enhancement," *Proceedings of the 43rd Annual Forum, American Helicopter Society*, Alexandria, VA (1987).

[3] D.F. Enns, "Multivariable Flight Control for an Attack Helicopter," *IEEE Control Systems Magazine* (April 1987).

[4] M.B. Tischler, "Digital Control of Highly Augmented Combat Rotorcraft ," NASA TM 88346, 1987.

[5] D.G. Miller & F. White, "A Treatment of the Impact of Rotor-Fuselage Coupling on the Helicopter Handling Qualities," *43rd Annual National Forum of the American Helicopter Society* (1987).

[6] R.H. Hoh, D.G. Mitchell & B.L. Aponso, "Proposed Specification for Handling Qualities of Military Rotorcraft. Vol. 1 - Requirements," USA AVSCOM Technical Report 89-A-4, May 1988.

[7] M.K.H. Fan, A.L. Tits, J. Barlow, N.K. Tsing, M. Tischler & M. Takahashi, "On the Design of Decoupling Controllers for Advanced Rotorcraft in the Hover Case," paper AIAA-91-0421, presented at the AIAA 29th Aerospace Sciences Meeting, Reno, Nevada, January 7-10, 1991.

[8] F.D. Kim, R. Celi & M.B. Tischler, "High-Order State-Space Simulation Models of Helicopter Flight Mechanics," *Proceedings of the 16th European Rotorcraft Forum*, Glasgow, UK (1990).

[9] M.K.H. Fan, L.-S. Wang, J. Koninckx & A.L. Tits, "Software Package for Optimization-Based Design with User-Supplied Simulators," *IEEE Control System Magazine* 9 (1989).

[10] M.K.H. Fan, A.L. Tits, J.L. Zhou, L.S. Wang & J. Koninckx, "CONSOL-OPTCAD User's Manual (Version 1.1, Released 9/1990)," Systems Research Center, University of Maryland, Technical Report TR-87-212r3, College Park, Maryland 20742, 1991.

[11] N.-K. Tsing, *Computer-Based Techniques for Control System Design, with Applications to Rotorcraft Control*, Ph.D. Dissertation, Dept. of Electrical Engineering, University of Maryland, College Park, 1992.

[12] "Rotorcraft Flight Control System Methodologies (part II)," Final report for NASA-Ames University Consortium Interchange #NCA2-510, 1992.

[13] M. Vidyasagar, *Control System Synthesis - A Factorization Approach*, MIT Press, 1985.

[14] S.P. Boyd & C.H. Barratt, *Linear Controller Design: Limits of Performance*, Prentice-Hall, Englewood Cliffs, NJ, 1991.

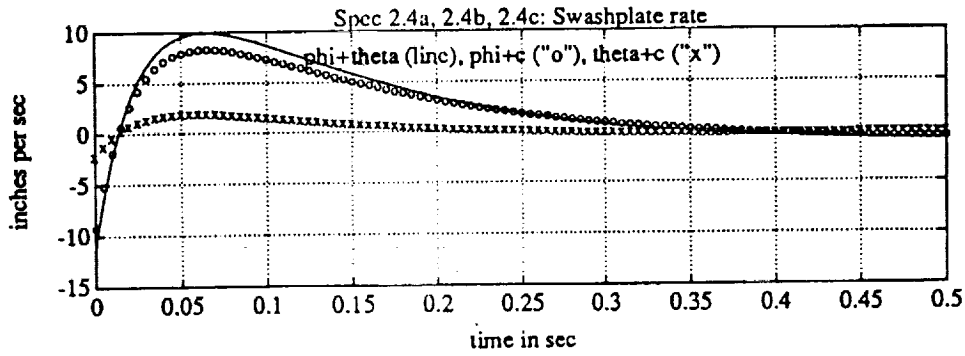

Figure 6. Pitch command: swashplate rates

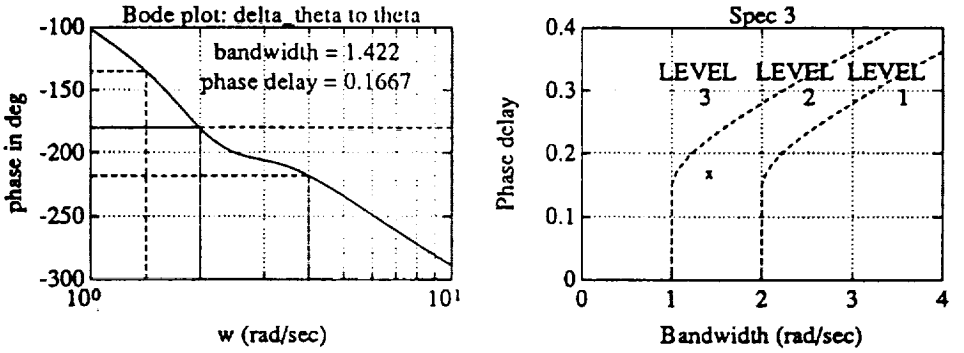

Figure 7. Bandwidth and phase delay for pitch channel

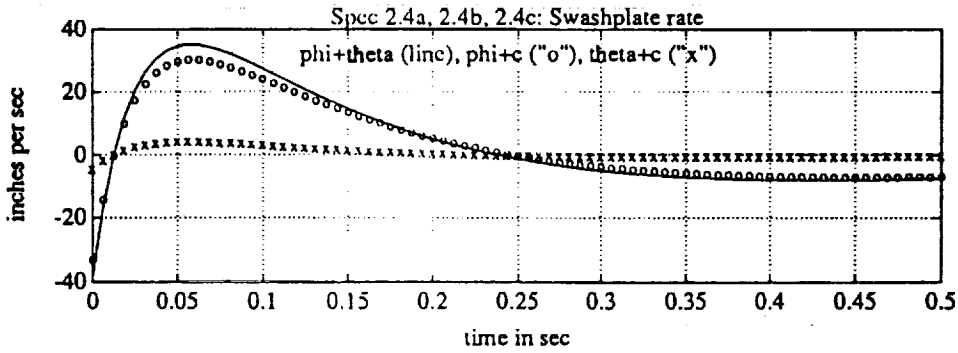

Figure 8. Pitch command: swashplate rates (alternate design)

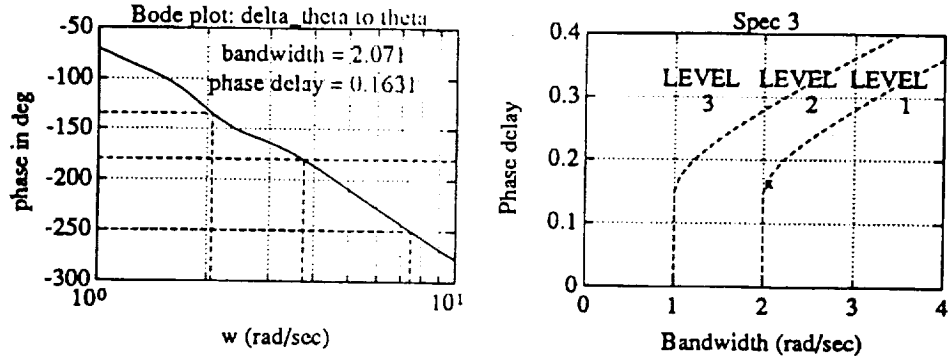

Figure 9. Bandwidth and phase delay for pitch command (alternate design)

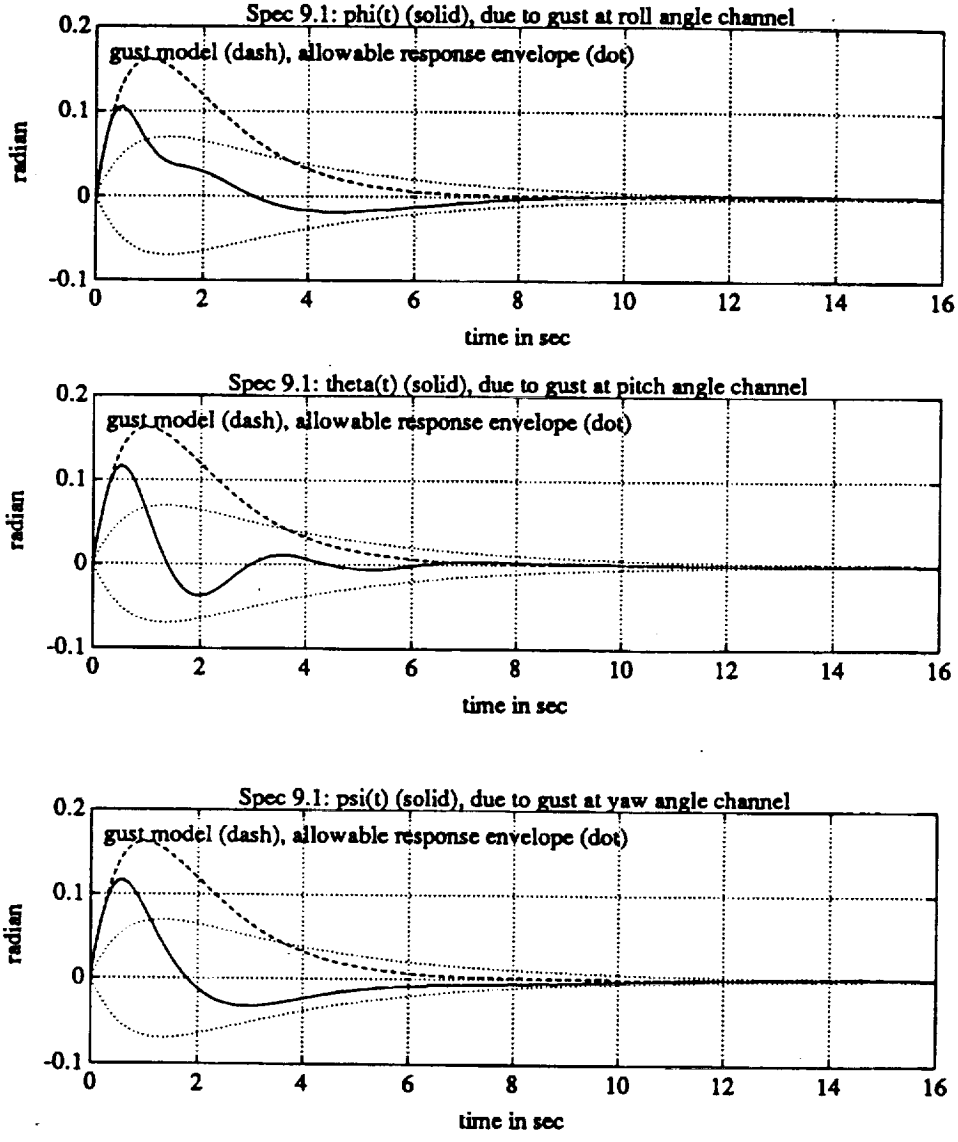

Figure 10. Time-responses to wind gust

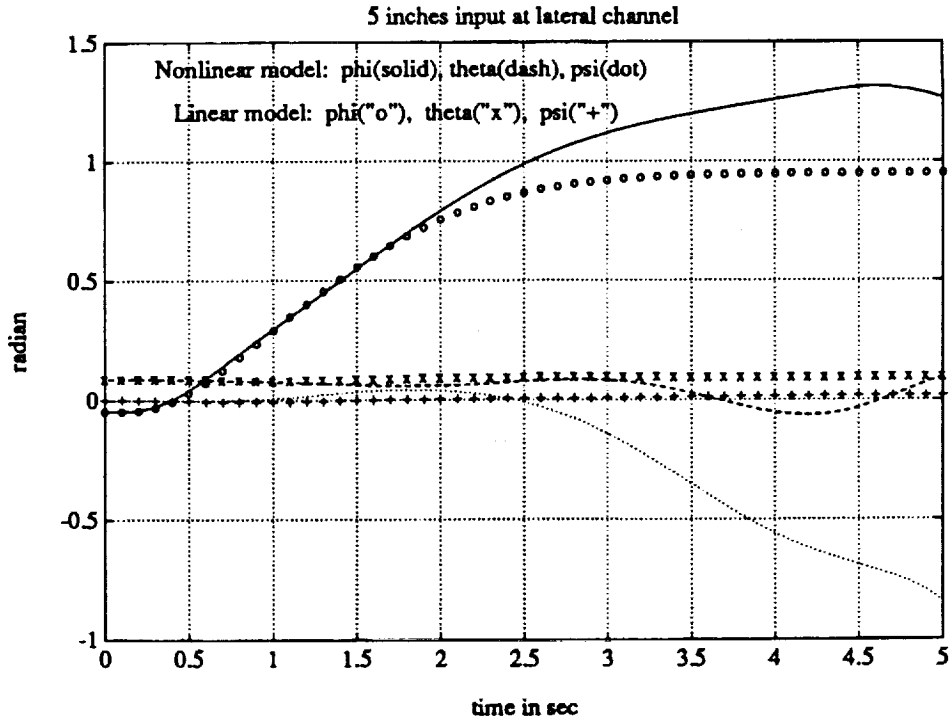

Figure 11. Nonlinear validation: large signals

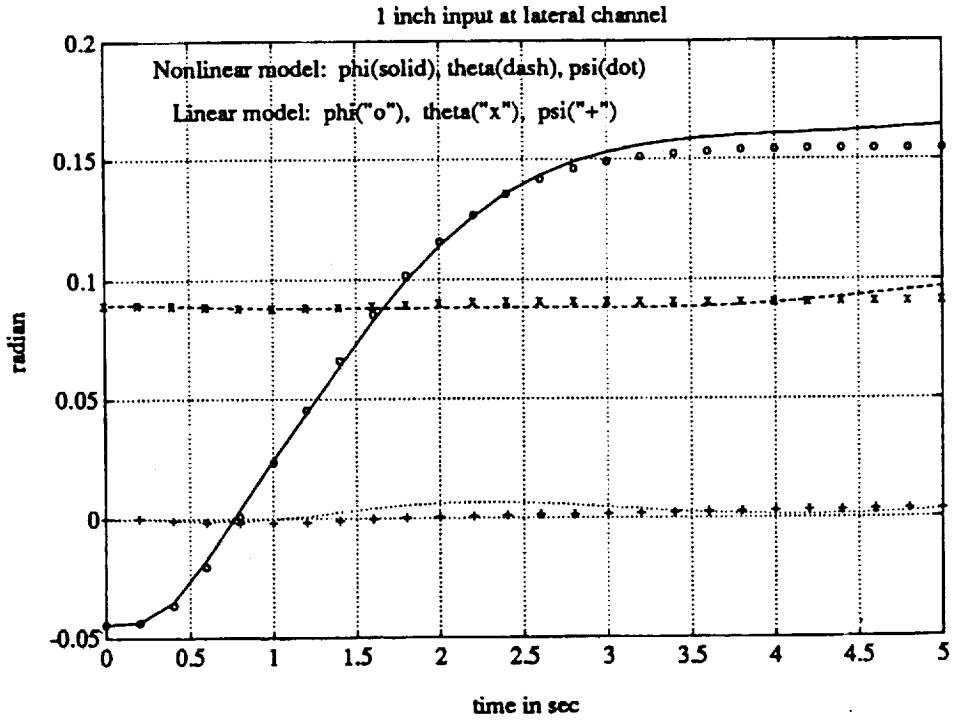

Figure 12. Nonlinear validation: average size signals

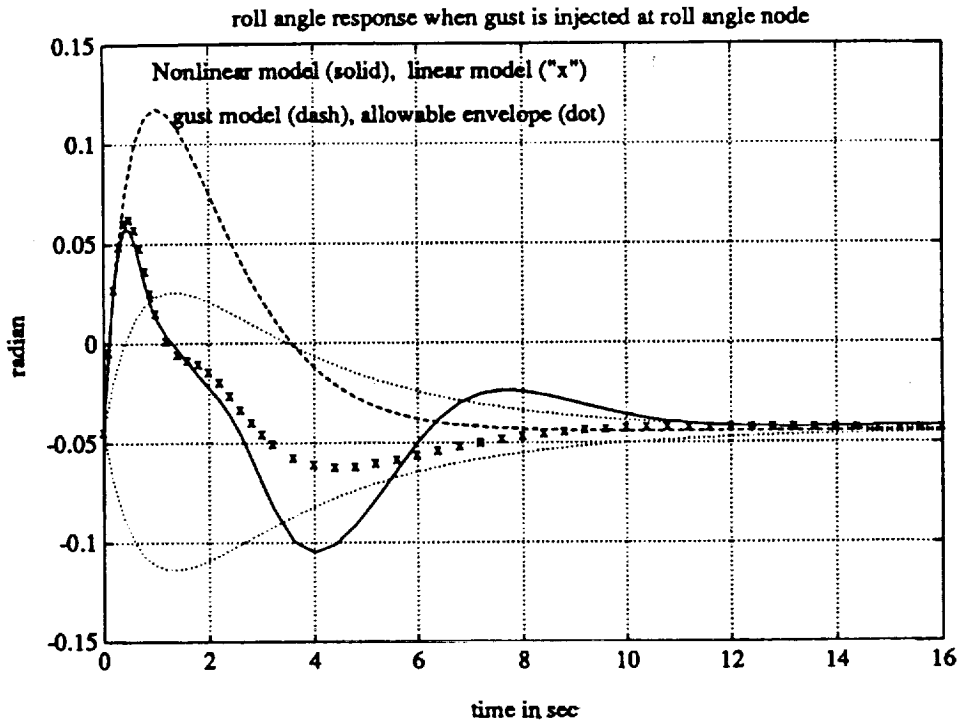

Figure 13. Nonlinear validation: wind gust rejection

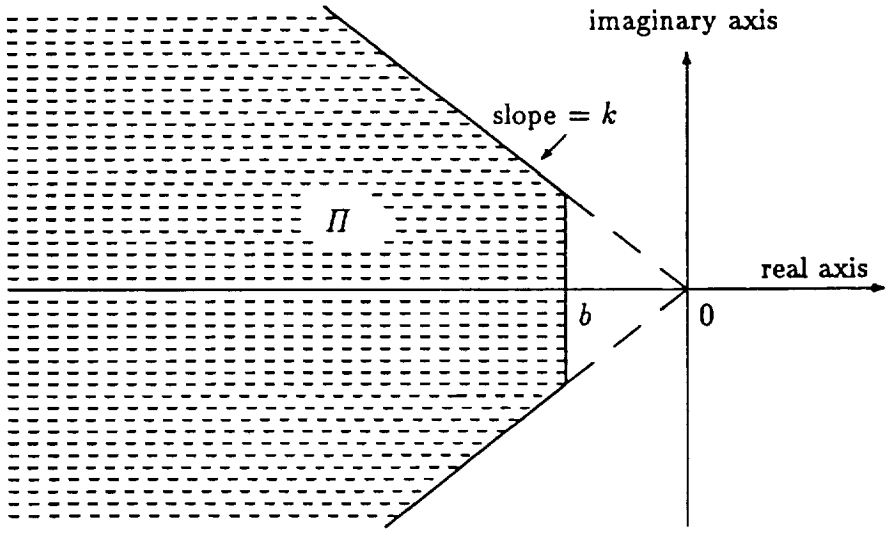

Figure 14. Π-stability region